JCARME
Journal of Computational and Applied Research in Mechanical Engineering
SRTTU
http://jcarme.srttu.edu
ISSN: 2228-7922
Vol. X, No. X, XXXX

Experimental Analysis of Shock Waves Turbulence in Contractions with Rectangular Sections

M.R. Nikpour[a], P. Khosravinia[b*] and D. Farsadizadeh[c]

[a] *Department of Water Engineering, University of Mohaghegh Ardabili, Ardabil, 9132220485, Iran*
[b] *Department of Water Sciences and Engineering, University of Kurdistan, Sanandaj, Kurdistan, 9120977875, Iran*
[c] *Department of Water Engineering, University of Tabriz, Tabriz, East Azerbaijan , 9143135801, Iran*

Abstract

Formation of shock waves has an important role in supercritical flows studies. These waves are often occurring during passage of supercritical flow in the non-prismatic channels. In the present study, the effect of length of contraction wall of open-channel for two different geometries (1.5 m and 0.5 m) and fixed contraction ratio was investigated on hydraulic parameters of shock waves using experimental model (models 1 and 2). For achieving to this goal, values of height and instantaneous velocity were measured in various points of shock waves observed in contractions for four Froude Numbers. In general, non-uniform distribution of velocity and turbulence intensity profiles were completely clear. Comparing results of models 1 and 2, show that the height and velocity values of formed waves in the model 2 is so much more than the model 1. Also, motion of the shock waves was accompanied with longitude gradient decrease of turbulence kinetic energy. The results of the present research can be very useful for designer engineers.

Keywords:

Contraction, Shock wave, Supercritical flow, Turbulence intensity, Turbulence kinetic energy.

Nomenclature

u	Instantaneous velocity component in the x- direction	Fr_1	Froude number for incoming flow
$\overline{u}$	average velocity component in the x- direction	$\overline{K}$	Water depth
u_1	average of flow velocity beneath the sluice gate	u'	Minor fluctuation of instantaneous velocity
X	longitude distance at the beginning of wave formation	**Abbreviations**	
z	vertical distance from the bed	*CSW*	Classic shallow water equations
d	opening of sluice gate	*ECSW*	Extended Classic shallow water equations
Q	Flow discharge	*CFD*	Computational fluid dynamic
H	Flow head	*VOF*	Volume of Fluid
y	Water depth		

[*] *Corresponding author*
Email address: p.khosravinia2012@gmail.com

1. Introduction

Open channels carrying supercritical flows are commonly used in hydraulic engineering applications. Man-made structures such as spillways chutes, conveyance channels, sewer systems, and outlet works are some typical examples. Similarly, supercritical flows occur in many natural channels, in mountainous streams and in rivers during periods of high flows [1]. Compared to subcritical flow, supercritical open channel flow is characterized by the formation of shock waves [2].

The transverse waves generated in fast flows of open channels are similar to shock waves in supersonic gases. Therefore, the transverse waves formed in supercritical flows are also known as shock waves. The presence of complications such as constriction, expansion, rising and lowering of bed level, bends and etc. in channels with supercritical flow conditions, will cause will cause a sudden change in the depth and velocity of the flow and subsequently the shock waves can form. In the study of supercritical flows, the formation of shock waves is of high importance.

Shock waves are generated in a supercritical flow channel due to changing cross section geometries, side wall deflection or small obstacles within the flow area and can cause damage to hydraulic structures and the surrounding environment unless they are considered during construction phase [3]. In a contraction, production of the shocks generates a disturbance pattern that can persist for a considerable distance downstream. However, if the transition is designed properly, the waves will not propagate in the downstream channel. Predicting the possible locations of oblique standing waves and determining the elevations of the water surface is necessary to design the required wall heights to avoid overtopping [4]. For the first, Von-Karman (1938) was able to derive the governing two-dimensional of supercritical flow in contractions using the CSW [2]. The analytical solution for the wave development in straight transitions is provided by Chow (1959) [5]. In the recent years, advanced numerical methods have been applied for studying shock waves in transitions. The unsteady, depth-averaged and two-dimensional shallow water equations to simulate transient free-surface flow under extreme boundary conditions have solved using finite difference method [6-7]. The suitability of the numerical scheme to predict different characteristic flow features are clearly demonstrated in their studies. Analysis of shallow water equations was carried out for numerical simulation of supercritical flow in sharp bends [8]. Analyzing flow profiles was done in subcritical and supercritical flows in an open channel that includes either a contraction in width, or a rise in bottom using the specific-energy concept [9].The CSW equations were extended to simulate supercritical flow in channel transitions including a modified Rouse channel expansion with a large approach flow Froude number (Fr_o=8), which was experimentally studied by Mazumder and Hager (1993) [10]. The solutions with the extended approach (ESWE) were compared both with a part of the available experimental data (only flow depths) and with the standard SWE. A 3-D CFD model based on the VOF method was utilized to calculate the free surface of supercritical flow in gradual open channel expansions [12]. A detailed comparison between the numerical and the experimental results concerning surface profiles and shock front location showed satisfactory agreement, especially for lower supercritical Froude numbers. An analytical model were developed to predict supercritical bend flow in a rectangular chute [13]. The proposed model was verified by comparing the results with the available experimental data and the reported theoretical expressions for the free surface profile along the outer chute wall. A novel method introduced for the reduction of wave height along the outer wall of a bend by adding a convex corner to the inner bend wall [14]. By using an optimized convex corner, the wave height may be reduced between 10 and 45%. Supercritical flow in curved open channels was simulated using three-dimensional CFD analysis [15]. The CFD analysis was carried out on two 45° curved open channels using the FLUENT. Overall results indicated that the model has an excellent prediction of flow pattern of supercritical bend flow and also the wave length and wave height in the

inner and outer wall of bends. The complex flow pattern occurring in a close conduit bend with supercritical flow condition was reported. They developed simple empirical relationship that describe the effects of the bend deflection angle and approach flow conditions on the considered flow [16].
Experimental and VOF-based CFD simulation concerning the impact of dam-break induced shock waves on a vertical wall at downstream end was investigated. Regarding numerical simulation, two distinct models including Reynolds- averaged Navier–Stokes equations (RANS) with the k-e turbulence model and the Shallow Water Equations (SWEs) were utilized. Comparison results good agreement between numerical simulation and observed data.[17]. The capability of a coupled 1D-2D model to simulate the flow processes during supercritical flows in crossroads was studied. They stated that the coupled 1D-2D model can be useful for reducing running time while preserving the solution accuracy and level of detail [18].
On the base of literatures and to the best of our knowledge, although the free surface profile in contraction was investigated but analysis of turbulence parameters has not been considered at the contraction location. In the present study, values of depth and instantaneous velocity were measured in various points of shock waves observed in contractions for four Froude numbers. In addition to analyzing of free surface and velocity profiles, turbulence parameters of shock waves including turbulence kinetic energy and turbulence intensity were investigated.

Materials and Methods

Experimental setup

The experiments of this research were conducted in the hydraulic laboratory at the University of Urmia, department of Water Engineering. The test facility comprised of a horizontal 6.0 m long, 0.7 m high and 1.0 m wide rectangular metal flume. A head tank with a length of 1.75 m, height of 1.20 m and width of 1.65 m supplied the discharge into the flume. The entrance discharge to the reservoir was set by a valve installed on the drift tube of pump. A steel sluice gate with a thickness of 3 mm and a height of 2.1 m was installed at entrance of the flume in order to regulate the water level and control the Froude number. During the tests, four sheets of plexy-glass with a thickness of 6 mm, a length of 1 m and a height of 30 cm were utilized to make upstream and downstream channels of transitions. Also, four sheets of plexy-glass with a thickness of 6 mm, length of 1.5 and 0.5 m and a height of 30 cm were utilized for walls of the transitions. A false floor made of compressed polyethylene with a thickness of 1 cm, a length of 3.5 m and a width of 1 m was placed at the beginning of the flume, in order to install the walls of the transitions and the upstream and downstream channels. In all experiments, opening of sluice gate was 2 cm and widths of upstream and downstream channels were considered 80 and 40 cm, respectively. The flow discharges were measured by an ultrasonic flow-meter having the accuracy of 0.02 lit/s. The wave heights in the section of contractions were measured at equally spaced intervals by a point gauge having the accuracy of 0.1 mm. An electromagnetic 2-D velocity meter was used for measuring of instantaneous velocity in various points of shock waves. The experiments were conducted for four Froude numbers including 3.2, 5.4, 7.0 and 9.1. It should be noted that the Froude number during the experiments were obtained by changing the water level in the tank head. Important flow parameters are listed in Table 1, where Q, H, y and Fr_1 are referred as the discharge, flow head, water depth and Froude number for incoming flow, respectively.

Table 1. Characteristics of the experiments.

Q (lit/s)	H (m)	y (m)	Fr_1
19.1	0.79	0.018	3.2
32.4	0.90	0.018	5.4

38.6	0.98	0.017	7.0
46.3	1.08	0.016	9.1

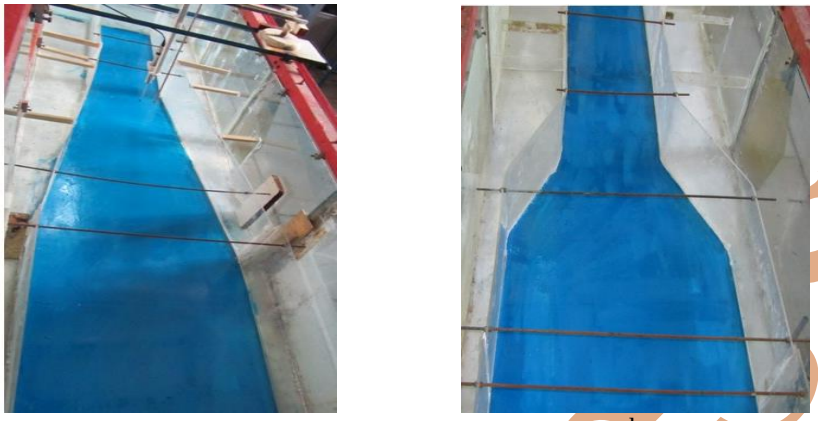

a b

Fig. 1. Upstream view of the contractions (a): model 1 (b): model 2

In order to investigate the effect of transition wall length on hydraulic parameters of the shock waves, two models of the contractions were used with straight walls and lengths of 1.5 and 0.5 m (model 1 and model 2). Figure 1 shows a view of the contractions used in this study.

After stabilizing the water level in the head tank for the Froude numbers in Table 1, with water passing under the sluice gate, supercritical flow was seen within the channel. Upon reaching the supercritical flow to the beginning of the transition, the shock waves start in diagonal form and collide with each other. Figures 2 and 3 show an example of the shock waves formed in the contractions for Fr_1=7.0.

Fig. 2. Formation of the shock waves in the model 1 for Fr_1=7.0

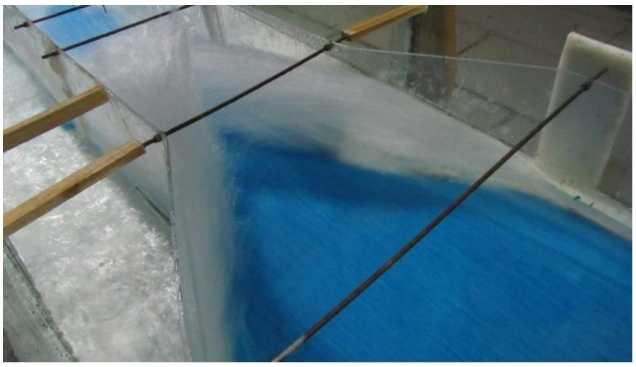

Fig. 3. Formation of the shock waves in the model 2 for Fr_1=7.0

After reaching a steady flow conditions and stability of wave's pattern in the contractions, values of instantaneous velocity were measured by the velocity meter along the wave's front from a distance of 10 cm from the beginning of the wave generation in five sections spaced 30 cm in length and 10 cm in the models 1 and 2. In addition to, in the model 1 values of velocity were measured in the vertical direction from a distance of 5 mm of the bed to 5 mm of the wave's surface at intervals of 5 mm, vertically.
For instance, the locations of instantaneous velocity measurements for model 2 are shown in Fig. 4.

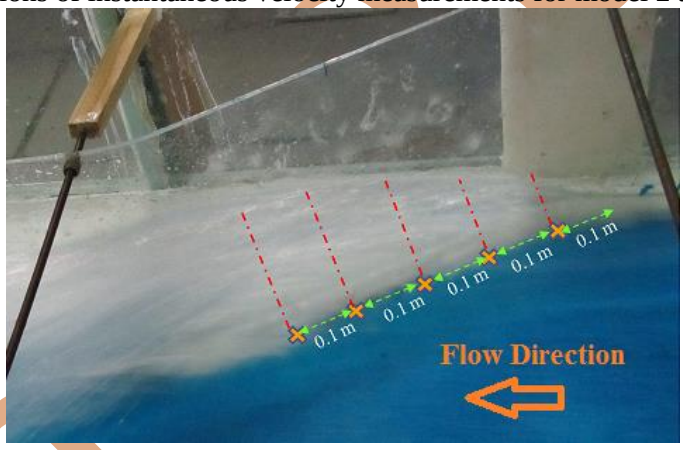

Fig. 4. The locations of instantaneous velocity measurements for model 2

As the same way, in the model 2 they were measured in the vertical direction from a distance of 5 mm of the bed to 1 cm of the wave's surface at intervals of 5 mm. At any point of the waves, 5 seconds was considered for velocity values measuring. Within that time, 100 components of instantaneous velocity (u) were recorded and average of them was considered for the target point ($\bar{u}$). As be mentioned, surface profiles of the shock waves were measured by the point gauge along the wave's front. Due to the high intensity of flow turbulence and mixing of water and air, there was risk of error when reading the wave surface profiles. In order to minimize the error, at each point the height was measured several times and average of them was recorded as wave height of the target point.

Results and Discussion

Analysis of height and velocity profiles of shock waves

Figures 5 and 6 show the velocity profiles of models 1 and 2 along the shock waves movement for the Froude numbers. X(m) demonstrates longitude distance at the beginning of wave formation (Figures 5 and 6). And z, d, u and $\overline{u_1}$ are indicate vertical distance from the bed, opening of sluice gate, instantaneous velocity in longitude direction and average of flow velocity beneath the sluice gate. Figures 7 and 8 show the free surface profiles of the models along the shock waves movement for the Froude numbers.

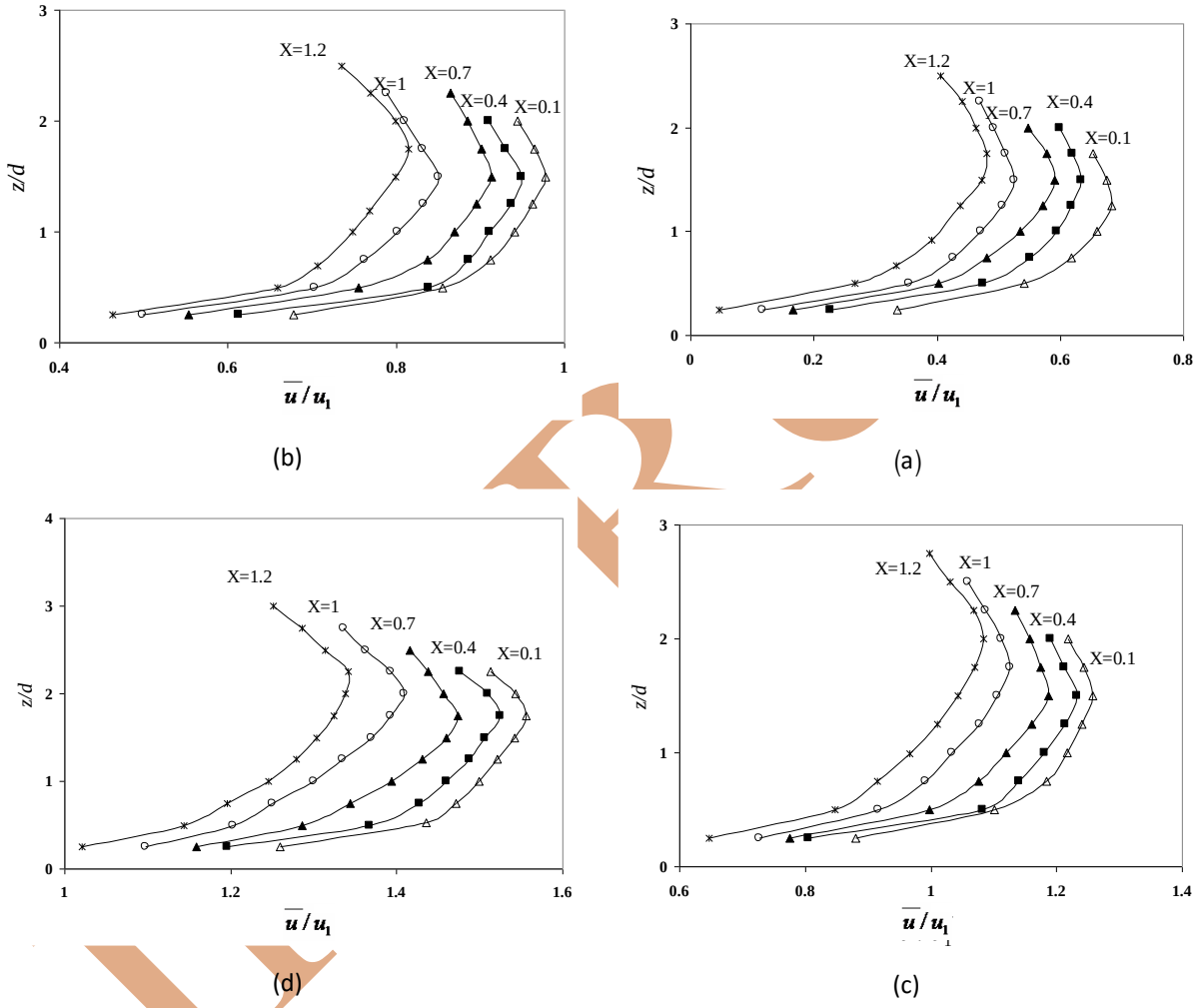

Fig. 5. Velocity profiles of shock waves in the model 1 for:
(a):Fr_1=3.2 (b):Fr_1=5.4 (c):Fr_1=7.0 (d):Fr_1=9.1

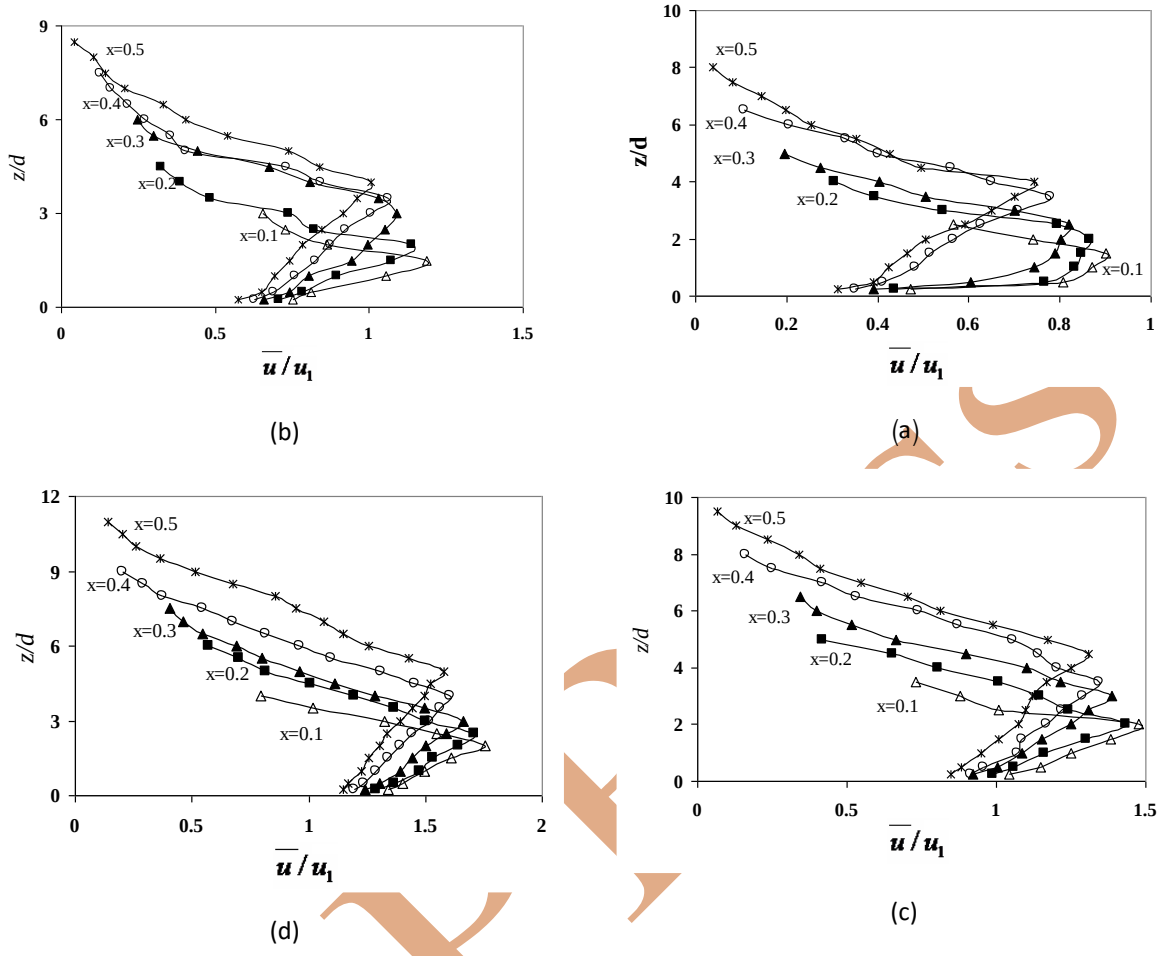

Fig. 6. Velocity profiles of shock waves in the model 2 for:
(a):Fr_1=3.2 (b):Fr_1=5.4 (c):Fr_1=7.0 (d):Fr_1=9.1

The measured values indicate non-uniform distribution of velocity in vertical direction of the shock waves. The velocity values increased from the bed and beganning to decrease after the maximum value reached. On the other hand, it intensifies by movement of the shock waves front and amplification of water and air mixture. In each velocity profile, two distinct regions can be considered: region of velocity increment (the first region) and region of velocity reduction (second region).

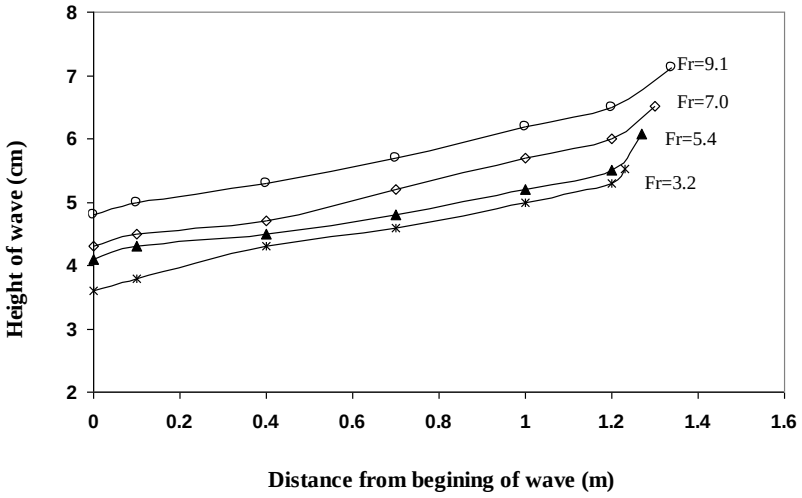

Fig. 7. Free surface profiles of the shock waves for the model 1.

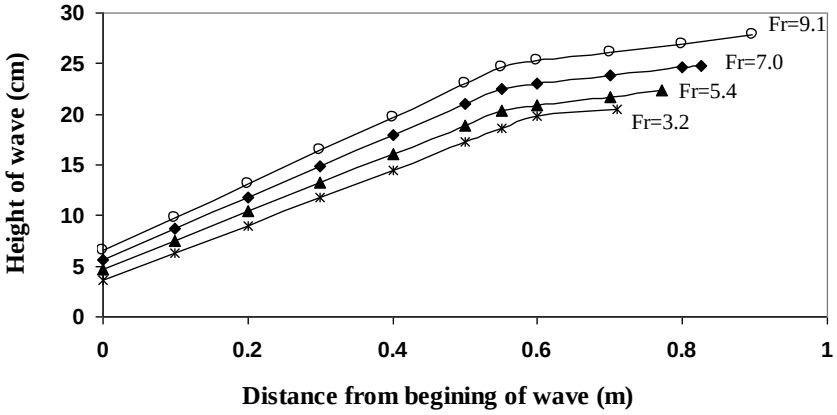

Fig. 8. Free surface profiles of the shock waves for the model 2.

Tables 2 and 3 show reduction values of wave velocity in models sections for X=0.1 and X=0.4. The values are calculated by subtracting velocity of wave surface from maximum velocity. Also, the results show that moving from wave front to downstream causes reducing velocity and increasing wave height. Actually, interface of the first oblique wave and channel mainstream was accompanied with dissipation of turbulence kinetic energy, increment of the shock wave height and reduction of its velocity.

Table 2. Velocity reduction (m/s) in the second region at X=0.1

Model	Fr_1=3.2	Fr_1=5.4	Fr_1=7	Fr_1=9.1
Number 1	0.075	0.085	0.096	0.108
Number 2	0.842	1.331	1.868	2.402

Table 3. Velocity reduction (m/s) in the second region at X=0.4

Model	Fr_1=3.2	Fr_1=5.4	Fr_1=7	Fr_1=9.1
Number 1	0.087	0.096	0.107	0.121
Number 2	1.681	2.336	2.954	3.508

comparing figures 5 and 6 and the results of tables 2 and 3, shows that velocity reduction in the second region of model 2 is much greater than model 1.One of the factors making shock waves in the supercritical flow, is reduction of channel width. This factor, in model 2 has been performed in a shorter distance than the model 1, so, fluid behavior changes in the model 2 is stronger than the model 1. Height and velocity of the shock waves of model 2 is bigger. The shock waves formed in the model 2 had mixture air and water stronger than the model 1 and this factor followed severe reduction of the wave velocity in the second region. By comparing the figures 7 and 8 can be seen that wave front height of the model 1 have increased with a mild slope, in the event that in the model 2, height of the shock waves have increased suddenly and after separating the wave front of the transition wall to the interface place of the waves, it was slowly increased. Given that in the model 1 width reduction of the channel has been carried out gradually and in the longer path than the model 2, therefore the shock waves formed in the model 1 have the less height and velocity than the model 2.

Analysis of turbulence kinetic energy

Figures 9 and 10 show turbulence kinetic energy changes of the shock waves along their movement for various Froude numbers in the models 1 and 2. In the figures $\overline{K}$ refers as average of turbulence kinetic energy in any vertical direction of the wave. Downward trend of the mentioned parameter is clear along the wave front. As be mentioned, interface of the first oblique wave and channel mainstream causes dissipation of turbulence kinetic energy. Longitudinal gradient reduction of turbulence kinetic energy for various Froude numbers in the models 1 and 2 are reported in the table 4. The mentioned values were achieved of difference between the values of turbulence kinetic energy at the beginning and end of the measuring points toward the length of the interval.

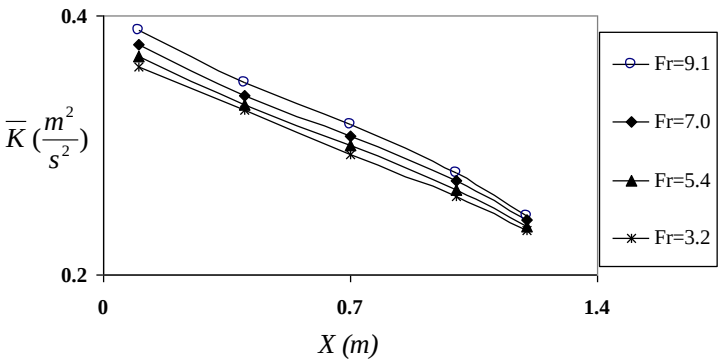

Fig. 9. Turbulence kinetic energy changes of the shock waves in the model 1.

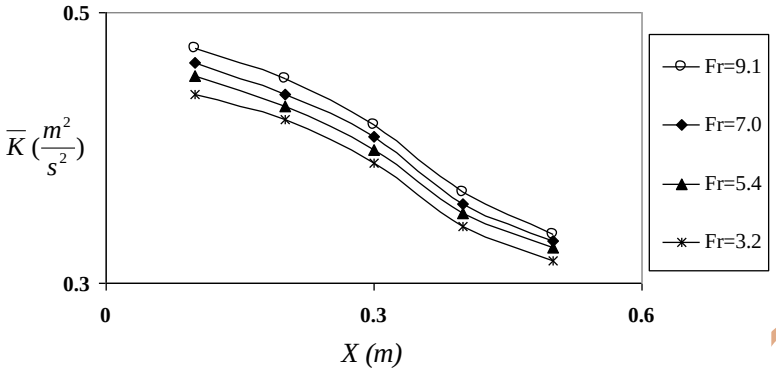

Fig. 10. Turbulence kinetic energy changes of the shock waves in the model 2.

Table 4. Longitudinal gradient reduction of turbulence kinetic energy ($m^2/s^2/m$)

Model	Fr_1=3.2	Fr_1=4.6	Fr_1=5.4	Fr_1=6.3	Fr_1=7	Fr_1=8.2	Fr_1=9.1
Number 1	0.115	0.117	0.120	0.123	0.124	0.127	0.131
Number 2	0.308	0.313	0.318	0.328	0.330	0.338	0.345

Analysis of turbulence intensity

Figures 11 and 12 show turbulence intensity changes of the shock waves along their movement for various Froude numbers in the models 1 and 2. In mentioned figures, u' indicates minor fluctuation of instantaneous velocity. It can be seen that turbulence intensity values of the model 1 have increased from the bed and began to decrease with a mild slope after reaching the maximum value, but model 2 have faced a sudden drop after the maximum value is reached, then reached a constant amount. This situation is more evident with wave development. As regards the mixing water and air causes fluctuations reduction of the instantaneous velocity and thereby is one of the reducing factors of turbulence intensity, therefore, decreasing the turbulence intensity values in all two models can be due to the mixing of water and air. On the other hand, as mentioned above intensity of mixing water and air in the shock waves of the model 1 was far less than the other model, so, turbulence intensity of the waves formed in this model is not faced with sensible drops. It was also observed that in model 2 accompanied with wave development and increase of its height, the corresponding z/d amount to the place of maximum turbulence intensity increases. But during the wave development in the model 1, its thickness has not changed significantly and thereby the place of maximum turbulence intensity does not have sensible change.

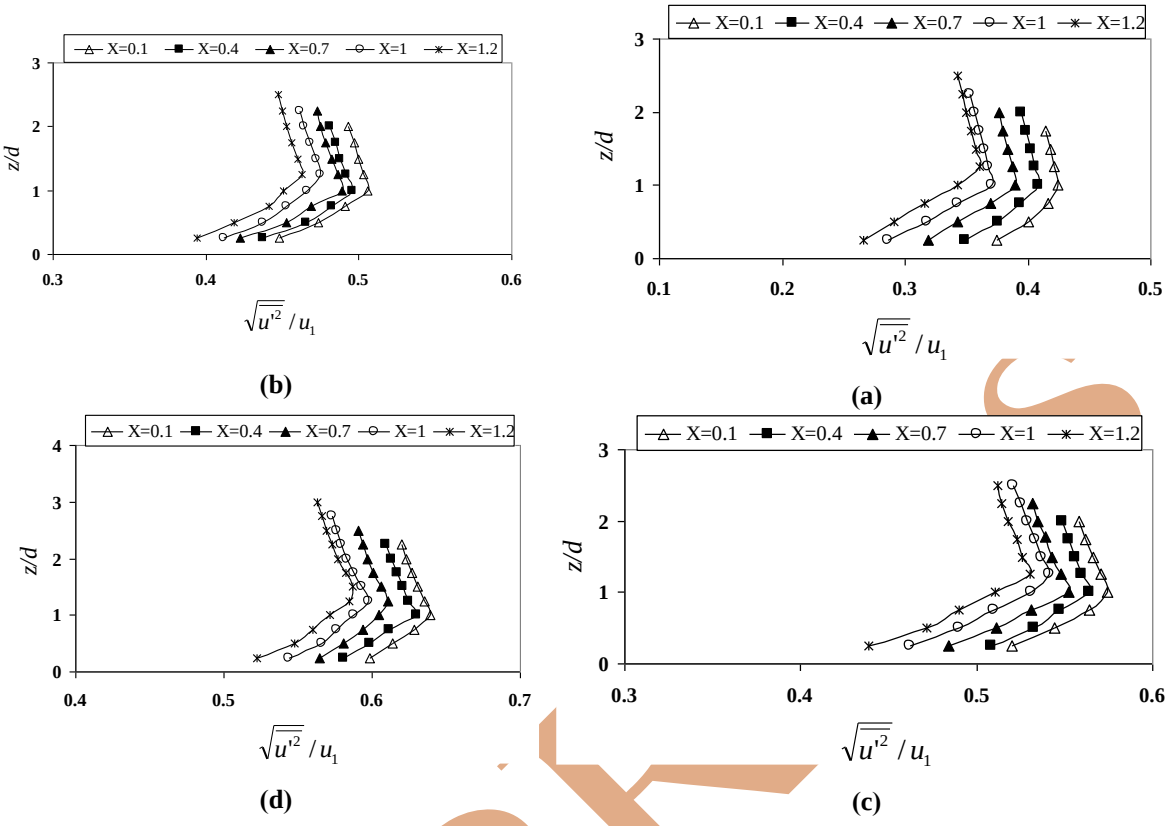

Fig. 11. Turbulence intensity profiles of shock waves in the model 1 for:
(a):Fr_1=3.2 (b):Fr_1=5.4 (c):Fr_1=7.0 (d):Fr_1=9.1

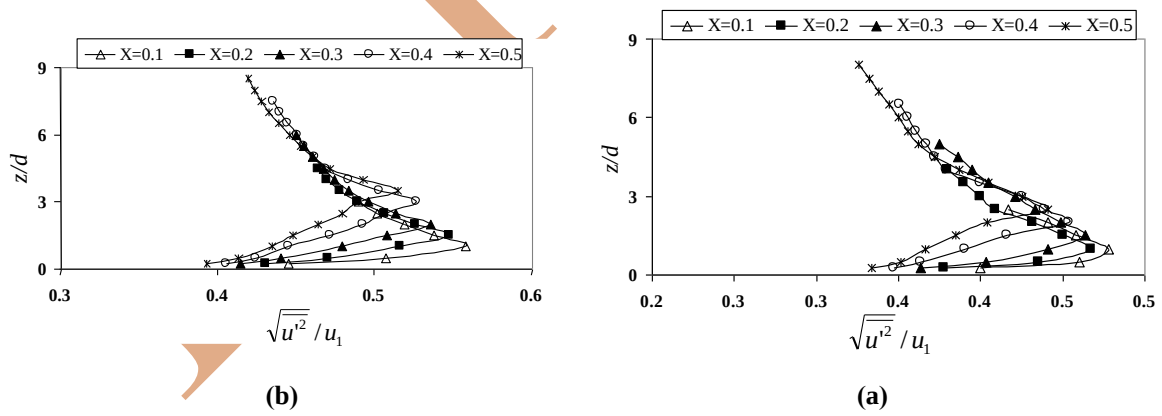

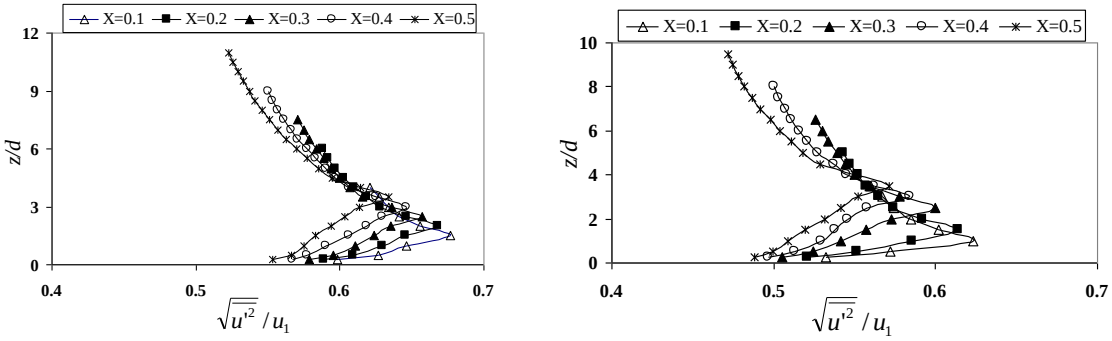

Fig. 12. Turbulence intensity profiles of shock waves in the model 2 for:
(a):Fr_1=3.2 (b):Fr_1=5.4 (c):Fr_1=7.0 (d):Fr_1=9.1

Conclusion

In this research, shock waves formation in open-channels contractions with rectangular sections was studied and the following results is obtained:

1. Distribution of velocity in vertical direction of the shock waves is not non-uniform, as, the velocity values increased away from the bed and began to decrease after reaching the maximum value because of mixing water and air in the wave surface.
2. Increase of the Froude number and development of wave front has increment impact on turbulence intensity of the wave and mixture of water and air. As a result, wave velocity decreased strongly in the second region. The reduction of velocity at a distance of 10 cm from location of wave formation and Froude number in the range of 3.2-9.1 in the model 1, was 0.075-0.018 whereas in the model 2 was 0.842-2.402 (m/s) that observed in the second region. Furthermore, the mentioned values at 40 cm from location of wave formation for models 1 and 2, were obtained as 0.087-0.121 and 1.681-3.508 (m/s), respectively.
3. Comparing results of models 1 and 2, shows that the height and velocity values of formed waves in model 2 is so much more than model 1. Also, amount of velocity reduction in the second region of model 2 was much greater than model 1. Sudden reduction of channel width that accompanied with rapid collision of channel flow to transition wall and amplification of mixing water and air caused the mentioned differences. The results of current study are in agreement with previous ones (i.e Jimenez and Chaudhry (1988), Bhallamudi and Chaudhry (1992) and Jain (1993)).
4. For a constant Froude number, longitudinal gradient reduction of turbulence kinetic energy in the model 2 was greater than the model 1. Although shock waves of the model 2 had more amount of turbulence kinetic energy than the model 1, but during mileage by the waves more energy dissipation was observed in this model. So that for Froude number in the range of 3.2-9.1 in the model 1, the reduction in the gradient of longitudinal kinetic energy of turbulence for models 1 and 2, were in the range of 0.115-0.131 and 0.308-0.345 ($m^2/s^2/m$), respectively.
5. Turbulence intensity values of the model 1 increased away from the bed and began to decrease with a mild slope after reaching the maximum value, but values of the model 2 after reaching the maximum value, faced with a sudden drop and then reached to a constant amount. Given that the mixing water and air causes fluctuations domain reduction of the instantaneous velocity, therefore, decreasing the turbulence intensity values in the models can be due to the mixing of water and air. It should be mentioned that turbulence intensity maximum was seen in the shock waves of the model 2.

6. Based on the results of this study recommends that designing the contractions in a state of supercritical flow, due to minimize height of shock waves and their destructive effects, the smallest convergence angle must be selected. If there is a restriction on the length of the transition wall before running the
7. prototype, formation of the shock waves must be investigated using experimental or numerical models.

References

[1] O. F. Jimenez, and M. H. Chaudhry, "Computation of supercritical free-surface flows", *J. Hydraulic Engineering* , Vol. 114, No. 4. pp. 377-395, (1988).

[2] W. H. Hager, "Supercritical flow in channel junction". *J. Hydraulic Engineering* , Vol. 115, No. 5. pp. 595-616, (1989).

[3] F. Feurich, and N. R. B. Olsen, "Finding Free Surface Of Supercritical Flows- Numerical Investigation". *J. Engineering Applications of Computational Fluid Mechanics*, Vol. 6, No. 2. pp. 307–315, (2012).).

[4] D. M. Causon, "Advances in calculation methods for supercritical flow in spillway channels" *J. Hydraulic Engineering*, Vol. 125, No. 10. pp. 1039-1050, (1999).

[5] V.T. Chow, *Open Channel Hydraulics*, McGraw-Hill Publisher, Michigan, (1959).

[6] R. J. Fennema, and H. M. Chaudhry, "Explicit methods for 2-D transient free-surface flows", *J. Hydraulic Engineering*, Vol. 116, No. 8. pp. 1013-1035, (1990).

[7] S. M. Bhallamudi, and M. H.Chaudhry, "Computation of flows in open-channel transitions", *J. Hydraulic Research*, Vol. 30, No. 1. pp. 77-93, (1992).

[8] A. Valiani, and V. Caleffi, "Brief analysis of shallow water equations suitability to numerically simulate supercritical flow in sharp bends". *J. Hydraulic Engineering*, Vol. 131, No. 10. pp. 912-916, (2005).

[9] S. C. Jain. "Nonunique water- surface profiles inj open channels". *Journal of Hydraulic Engineering*, Vol.119, No. 12.pp. 1427-1434. (1993).

[10] S. Krüger, and P. Rutschmann, "Modeling 3D supercritical flow with extended shallow-water approach", *J. Hydraulic Engineering*, Vol. 132, No. 9, pp. 916-926, (2006).

[11] S. K. Mazumder, and W. H. Hager, "Supercritical expansion flow in Rouse modified and reversed transitions", *J. Hydraulic Engineering*, Vol. 119, No. 2, pp. 201-219, (1993).

[12] A. Stamou, D. Chapsas, and G. Christodoulou, "3-D numerical modeling of supercritical flow in gradual expansions", *J. Hydraulic Research*, Vol. 46, No. 3, pp. 402-409, (2008).

[13] M. Hessaroeyeh, and A. Tahershamsi, "Analytical model of supercritical flow in rectangular chute bends", *J. Hydraulic Research*, Vol. 47, No. 5, pp. 566-573, (2009).

[14] M. R. Jaefarzadeh, A. Shamkhalchian, and M. Jomehzadeh, "Supercritical flow profile improvement by means of a convex corner at a bend inlet", *J. Hydraulic Research*, Vol. 50, No. 6, pp. 623-630, (2012).

[15] M. Montazeri Namin, R. Ghazanfari-Hashemi, and M. Ghaeini-Hessaroeyeh, "3D numerical simulation of supercritical flow in bends of channel", *Int. Conference "Mechanical, Automotive and Materials Engineering"*, Dubai, United Arab Emirates, pp. 167-171, (2012).

[16] Kolarević, M., Savić, L., Kapor, R., & Mladenović, N. Supercritical flow in circular pipe bends. *Fme Transactions*, *42*(2), pp.128-132. (2014)

[17] Kocaman, S., & Ozmen-Cagatay, H. Investigation of dam-break induced shock waves impact on a vertical wall. *Journal of Hydrology*, *525*,pp. 1-12. (2015)

[18] Ghostine, R., Hoteit, I., Vazquez, J., Terfous, A., Ghenaim, A., & Mose, R.. Comparison between a coupled 1D-2D model and a fully 2D model for supercritical flow simulation in crossroads. *Journal of Hydraulic Research*, *53*(2),pp. 274-281. (2015)